



Production of Styrene-[Ethylene-(Ethylene-Propylene)]-Styrene Block Copolymer (SEEPS) Microfibers by Electrospinning

**OZAN TOPRAKCI^{1,2}, MUKADDES SEVVAL CETIN^{1,2}
and HATICE AYLIN KARAHAN TOPRAKCI^{*1,2}**

¹Yalova University, Faculty of Engineering, Department of Polymer Materials Engineering, 77100, Yalova, Turkey.

²Yalova University, Institute of Graduate Studies, 77100, Yalova, Turkey.

Abstract

Thermoplastic elastomer-based fibers have many advantages including lightness, flexibility, resilience. Styrene-[ethylene-(ethylene-propylene)]-styrene (SEEPS) is a styrenic block copolymer based thermoplastic elastomer and it can be used for many applications with many functions as a matrix, compatibilizer, modifier or adhesive. It has good resistance to oxidizing agents, weathering, aging, and it can be used under various conditions. In this study, SEEPS block copolymer fibers were electrospun. This study is the first study about the electrospinning of SEEPS block copolymer in the literature. Various spinning solutions were used, and process was optimized by changing the electrospinning conditions. Fiber morphology was analyzed by an optical microscope and fiber diameter distribution histograms were drawn. In order to understand the effects of polymer concentration on electrospinning, viscosity of the spinning solutions was measured. Although electrospinning conditions were found to be critical in terms of spinnability, solution concentration and viscosity were the most significant factors for obtaining flexible SEEPS based fibrous nonwoven mats.



Article History

Received: 04 January 2021

Accepted: 16 April 2021

Keywords

Electrospinning;
Microfibers;
SEEPS;
Thermoplastic Elastomers.

Introduction

Thermoplastic elastomers (TPEs) are rubbery materials that are basically mixture of thermoplastics and rubbers. In other words, they have both rubbery and thermoplastic phases together and they are

generally found as block copolymers. While the hard segments of the blocks are thermoplastic phase, soft segment of the blocks represent rubbery phase. Since hard segments function as physical cross-linking centers, TPEs do not require vulcanization.

CONTACT Hatice Aylin Karahan Toprakci ✉ aylin.toprakci@yalova.edu.tr 📍 Yalova University, Faculty of Engineering, Department of Polymer Materials Engineering, 77100, Yalova, Turkey.



© 2021 The Author(s). Published by Enviro Research Publishers.

This is an Open Access article licensed under a Creative Commons license: Attribution 4.0 International (CC-BY).

Doi: <http://dx.doi.org/10.13005/msri/180104>

Based on the ratio of the blocks, mechanical, morphological and processing properties of the TPEs change. Depending on the type of the hard segment, they can be classified as urethane, amide, olefin and styrene based TPEs. In all these types, styrene based thermoplastic elastomers offer unique properties including thermal, UV and aging resistance. The most common styrene based TPEs can be given as styrene-butadiene-styrene (SBS), styrene-isoprene (SI), styrene-isoprene-styrene (SIS) and poly[styrene-*b*-(ethylene-co-butylene)-*b*-styrene] (SEBS).¹ Also, styrene block copolymer microfibers can be produced by electrospinning. In the literature, many styrene block copolymers, i.e., poly(styrene-block-dimethylsiloxane),² poly(styrene-block-poly(4-vinylpyridine)),³ SI,⁴⁻⁵ SIS,⁵⁻⁶ SBS,⁷⁻⁹ and SEBS¹⁰ have been used to obtain sub-micron or microfibers by electrospinning. Although these polymers are promising for various applications, relatively new styrene-based block copolymer known as styrene-[ethylene-(ethylene-propylene)]-styrene (SEEPS) shows a growing attention recently.

High tensile strength, flexibility, shock absorption properties, resilience, low temperature performance, and good electrical insulation capacity make SEEPS advantageous. SEEPS is a hydrogenated styrenic block copolymer that can be used for various applications from automotive industry to household items and toys to cables as matrix, compatibilizer, modifier or adhesive. Since SEEPS does not contain double bonds in its chemical structure, it has good resistance to oxidizing agents, weathering, aging and can be used under extreme conditions. Although SEEPS is available in the market for more than 15 years, scientific literature about SEEPS is scarce. In most of these studies, blends were prepared and characterized. SEEPS was blended with polyamide (PA),¹¹⁻¹³ polyethylene terephthalate (PET),¹⁴ polypropylene (PP),¹⁵⁻¹⁸ PP/polystyrene (PS).¹⁹ In these studies SEEPS was generally used as an impact modifier or a compatibilizer. Depending on the ratio and type of the SEEPS enhancement in the mechanical properties were reported. In addition to SEEPS blends, composites were also studied.²⁰ In this study, magnetorheological properties of the SEEPS based isotropic and anisotropic composites were investigated. Also, various oils were also mixed with SEEPS in order to modify the morphology. As reported in these studies, depending on the oil type and amount viscoelastic properties varied.²¹⁻²³

Also there were couple of studies about understanding the morphology of SEEPS²⁴⁻²⁵ and crosslinking behavior of SEEPS.²⁶ These studies are of significance in terms of understanding morphology of SEEPS.

Electrospinning is a common method used for fabrication of ultra-fine, lightweight, pliable, flexible fibrous structures that have relatively high surface area and porosity. Depending on the polymer, solvent and processing conditions, various morphologies can be obtained. Although there are many studies in literature most of them were about electrospinning of thermoplastic polymers.²⁷⁻²⁸ The number of the studies about electrospinning of TPEs are relatively limited and in these studies, TPU was commonly used.²⁹⁻³¹ As mentioned above, there is no study about electrospinning of SEEPS block copolymer in literature.

In this study, SEEPS block copolymer was electrospun. Various spinning solutions were prepared, and optimization of the process was carried out. Viscosity of the spinning solutions was measured. Fiber morphology was analyzed, and fiber diameter distribution values were determined.

Materials and Method

Materials

In the study, SEEPS block copolymer with 30% styrene content was used (SEPTON 4033, Kuraray Co Ltd., Japan). The solvents, chloroform and toluene, were bought from Merck (Germany). All chemicals were used as received.

Preparation of Electrospinning Solution

The electrospinning solutions with the polymer concentration of 8, 10, 12 and 15 wt% were prepared. According to Flory-Huggins solubility mixing theory, small difference between solvent and polymer solubility parameters results in small enthalpy change. Gibbs free energy change in the mixing process comes closer to zero or negative values and mixing occurs. SEEPS block copolymer can be dissolved in many organic solvents including toluene, chloroform, hexane, cyclohexane, tetrahydrofuran, carbon tetrachloride, carbon disulfide etc. Among these solvents, toluene and chloroform have similar solubility parameter values, δ_{toluene} : 18.32 and $\delta_{\text{chloroform}}$: 18.94 MPa^{1/2}, respectively.³² Solubility parameters of styrene-

based copolymers are δ_{SEBS} : 15.7 MPa^{1/2},³³ δ_{SIS} : 16.84 MPa^{1/2},³⁴ and δ_{SB} : 17.5 MPa^{1/2}.³⁵ There is no study about solubility parameter of SEEPS (δ_{SEEPS}) in the literature, but it can be assumed as a value between 17.49 and 19.07 MPa^{1/2}.³⁶ Due to small difference between solubility parameters of SEEPS and toluene/chloroform, it can be said that toluene and chloroform are good solvents for SEEPS. In addition to solubility parameters of solvents, boiling temperature and vapor pressure of the solvents were taken into consideration for solvent selection for electrospinning. Toluene has higher boiling point (T_b :110.6°C) and lower vapor pressure (P_{vapor} : 2.8 kPa at 20°C) than chloroform (T_b : 61.2°C, P_{vapor} : 21.08 kPa at 20°C). During electrospinning, use of hardly boiling solvent is required in order to prevent clogging at the tip of the needle. On the other hand, collected electrospun fiber

on the collector should be dry enough to prevent the merging of the fibers. In other words, solvents used for the preparation of electrospinning solution should be completely evaporated between tip and collector. For all these reasons, the electrospinning solvent was chosen as a mixture of chloroform and toluene. Chloroform was chosen because of its higher volatility compared to toluene. Different weight ratios of chloroform to toluene (C:T = 8:2, 6:4, 4:6 and 2:8) were studied in order to optimize the electrospinning process parameters. For all solvent/polymer mixtures, spinning solutions were prepared by using a magnetic stirrer at 50°C until obtaining homogenous and clear solution. During optimization studies electrospinning performance and fiber formation were considered and based on those findings solvent ratio was determined as C:T=8:2.

Table 1: Electrospinning solution properties, electrospinning conditions, average fiber diameter, and standard deviation values of SEEPS fibers

Sample Code	Polymer Concentration (wt%)	Viscosity (cP)	Needle-collector Distance (cm)	Applied Voltage (kV)	Feed Rate (mL h ⁻¹)	Fiber Formation	Average Fiber Diameter (µm)	Standard Deviation (µm)
S1	8	196	15	15	0.25	No	-	-
S2					0.50	No	-	-
S3					0.75	No	-	-
S4					1.00	No	-	-
S5	10	625	15	15	0.25	No	-	-
S6					0.50	No	-	-
S7					0.75	No	-	-
S8					1.00	No	-	-
S9					1.50	No	-	-
S10					2.00	No	-	-
S11	12	1614	15	15	3.00	Yes	18.9	9.9
S12					0.25	No	-	-
S13					0.50	Yes/Clog	8.4	3.5
S14					0.75	Yes/Clog	13.1	6.0
S15					1.00	Yes/Clog	20.9	10.1
S16					2.00	Yes/Clog	23.4	10.3
S17					3.00	Yes/Clog	23.6	17.4
S18					15	2044	15	15
S19	0.50	Yes	7.1	1.7				
S20	0.75	Yes	9.1	1.5				
S21	1.00	Yes	9.2	1.6				
S22	2.00	Yes	23.8	6.0				
S23	3.00	Yes	24.1	6.7				

Electrospinning Process

Electrospinning of SEEPS was carried out by using a pump (New Era Pump Systems, NE-300, USA), a flat circular plate collector with 110 mm diameter, and a high voltage power supply (TN, ESPS-P303, China) (Fig.1). The volume of the syringe was 10 mL and the gauge of the needle was 21Gx2". The temperature was set to $29 \pm 1^\circ\text{C}$, and the humidity

was between 20-22% RH. Feed rate was changed in the range of $0.25\text{-}3\text{ mL h}^{-1}$. The voltage (15 kV) and the needle-collector distance (15 cm) were kept constant. Electrospinning solution concentration, solution viscosity, electrospinning conditions (feed rate, needle-collector distance, applied voltage) and average fiber diameter values can be seen from Table 1.

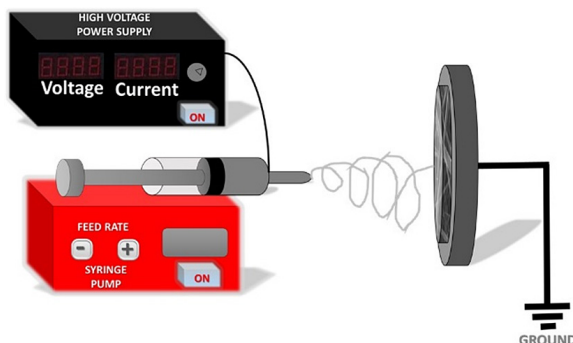


Fig. 1: Schematic illustration of electrospinning system

Characterization

Brookfield DV2T viscometer (USA) was used in order to determine the viscosity values of the spinning solutions. The measurements were done at 50 rpm with the spindle #4 at room temperature (25°C). The average value was calculated after three measurements were taken. The optical images of the electrospun fibers were analyzed by an optical microscope (BX51M, Olympus, Japan) under dark field mode. Image J software was used in order to determine average fiber diameter and fiber distribution histograms were drawn (around 200 different spots were selected in each image).

Results and Discussion

Solution Viscosity

Since viscosity is an indication of resistance to flow, it is significant not only for fiber formation but also for fiber morphology. In this study, three different spinning solutions were prepared as 8, 10, 12, and 15 wt% in order to determine the optimum polymer concentration. Viscosity of the solutions was determined by a viscometer under the same conditions. Normalized viscosity (NV) values were calculated in order to show the extent of increase in solution viscosity with increasing polymer concentration. NV values were determined by using the equation $(NV = \eta/\eta_8)$. η was the viscosity of the solution and η_8 was the viscosity of 8 wt%

solution. These values can be seen from Table 1. 8, 10, 12, and 15 wt% SEEPS containing solutions had viscosity values 196, 625, 1614 and 2044 cP, respectively. NV values of the samples were 1, 3.19, 8.23 and 10.42. As expected, increase in polymer concentration led to increase in viscosity. This rapid increase in viscosity is parallel with the literature. And, this was probably caused by higher level of inter- or intra-molecular interactions (i.e., increased entanglement) between polymer macromolecules.³⁷ In our case, the level of increase was also critical. While relative change was around 319% between 8 and 10 wt% SEEPS containing solutions, the value showed a dramatic increase between 8 and 15 wt% and was calculated as 1042%.

Morphology

In order to observe the fiber formation and morphology, samples were analyzed by an optical microscope. As seen from Fig. 2 and 3, fiber formation was not observed under all conditions. Fig. 2 shows morphologies of S1-S4 that were obtained from 8 wt% SEEPS solution at different electrospinning conditions. The processing conditions were as follows: Applied voltage was 15 kV, needle-collector distance was 15 cm and feed rates were 0.25, 0.5, 0.75 and 1 mL h^{-1} from S1 to S4, respectively. Effect of feed rate on fiber formation was studied. As obvious from Fig. 2, at this polymer concentration fiber

formation was not observed. Increase in feed rate led to higher amount of sprayed polymer on the collector. This was probably caused by low solution viscosity. At this value, entanglement and cohesion between

the polymer chains were not enough to stand electrical field. As a result of this, solution could not turn into fiber jet, instead, it was sprayed onto the collector regardless of the feed rate.

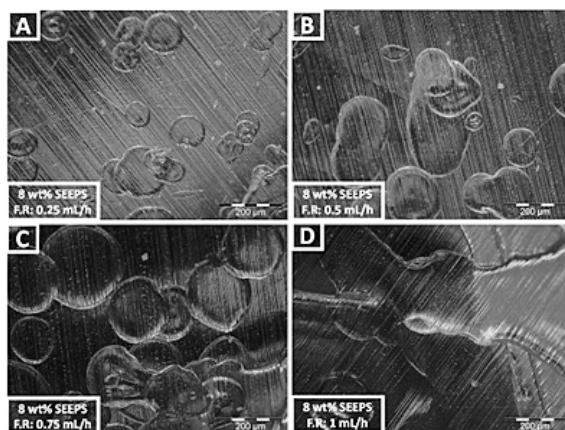


Fig. 2: Optical microscope images of electrospun samples from 8 wt% SEEPS solution (S1-S4) at 50x under different feed rates *F.R: Feed rate

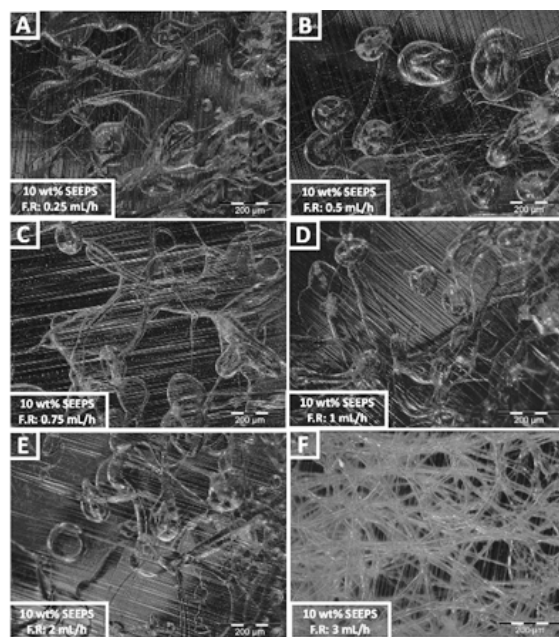


Fig. 3: Optical microscope images of electrospun samples from 10 wt% SEEPS solution (S5-S11) at 50x under different feed rates. *F.R: Feed rate

Fig. 3 shows S5-S11 that were obtained from 10 wt% SEEPS solution. The processing conditions were as follows: Applied voltage was 15 kV, needle-collector distance was 15 cm and feed rates were 0.25, 0.5, 0.75, 1, 2 and 3 mL h⁻¹. Parallel

with the previous step, the effect of feed rate on fiber formation was also studied. As obvious from Fig. 3, at 10 wt% polymer concentration, fiber formation was not observed at 0.25, 0.5, 0.75, 1, 2 mL h⁻¹ feed rate. However, the obtained

morphologies on the collector were different than the samples given in Fig. 2. As can be seen from Fig. 3, instead of drops in Fig. 2, fibrous drops were obtained. This was assumed to be caused by the increase in solution viscosity. As previously mentioned above, the solution viscosity of the S5-S11 was around three times higher than as S1-S4. As a result of this, entanglement and cohesion between polymer macromolecules increased and solution started to turn into non-continuous jets in

the electrical field. By increasing the flow rate to 3 mL h^{-1} , continuous jet formation and smooth fiber morphology were observed. Increase in feed rate led to higher amount of polymer solution between needle and collector that could stand the electrical field. However, fibers were merged from the contact points and solvent was not removed completely before fiber jet reached to the collector. The average fiber diameter of the S10 was calculated as $18.9 \mu\text{m}$.

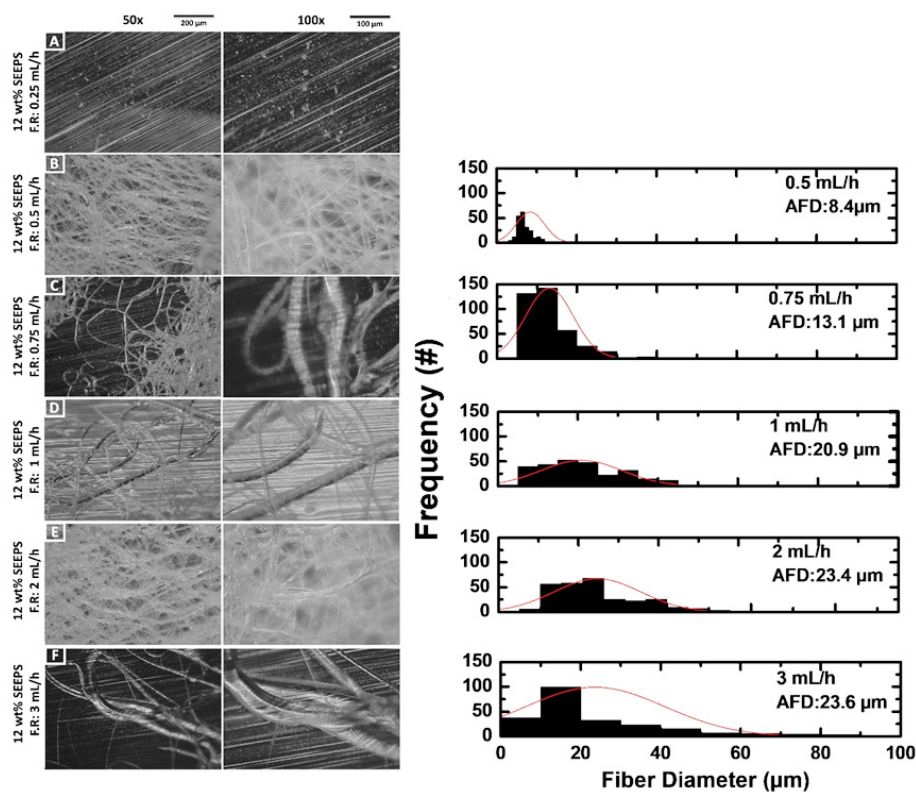


Fig. 4: Optical microscope images of electrospun samples from 12 wt% SEEPS solution (S12-S17) at 50x and 100x under different feed rates and corresponding fiber diameter distribution histograms. *F.R: Feed rate, *AFD: Average fiber diameter

Fig. 4 shows S12-S17 that were electrospun from 12 wt% SEEPS solution. Electrospinning was carried out under 15 kV with the needle-collector distance of 15cm and feed rates were 0.25, 0.5, 0.75, 1, 2 and 3 mL h^{-1} . As obvious from Fig. 4, no fiber formation was observed at 0.25 mL h^{-1} . Since the amount of spinning solution was relatively lower at this feed rate, spraying effect was observed. By increasing the flow rate to 0.5 mL h^{-1} , fiber formation was observed. The average fiber diameter was $8.4 \mu\text{m}$. From this

point any increase in feed rate led to increase in average fiber diameter. $0.75, 1, 2$ and 3 mL h^{-1} feed rate resulted in average fiber diameter $13.1, 20.9, 23.4, 23.6 \mu\text{m}$, respectively. Increase in the fiber diameter was probably caused by the higher amount of fiber solution between needle and collector.

Fig. 5 shows S18-S23 that were obtained from 15wt% SEEPS solution. The process parameters were kept the same for all sets. Applied voltage was 15 kV,

needle-collector distance was 15cm and feed rates were 0.25, 0.5, 0.75, 1, 2 and 3 mL h⁻¹. As obvious from Fig. 5, at 15 wt% polymer concentration, fiber formation was observed regardless of the feed rate. This was caused by the drastic increase in viscosity. As given in Table 1, viscosity of the 15 wt% was nearly 10.40, 3.26 and 1.26 times higher than that of 8, 10 and 12 wt% SEEPS

containing solutions, respectively. Higher polymer concentration led to higher interaction between polymer chains that increased the entanglement ratio and cohesion between macromolecules. 15 wt% polymer concentration was determined as the optimum solution for this type of SEEPS under given electrospinning conditions.

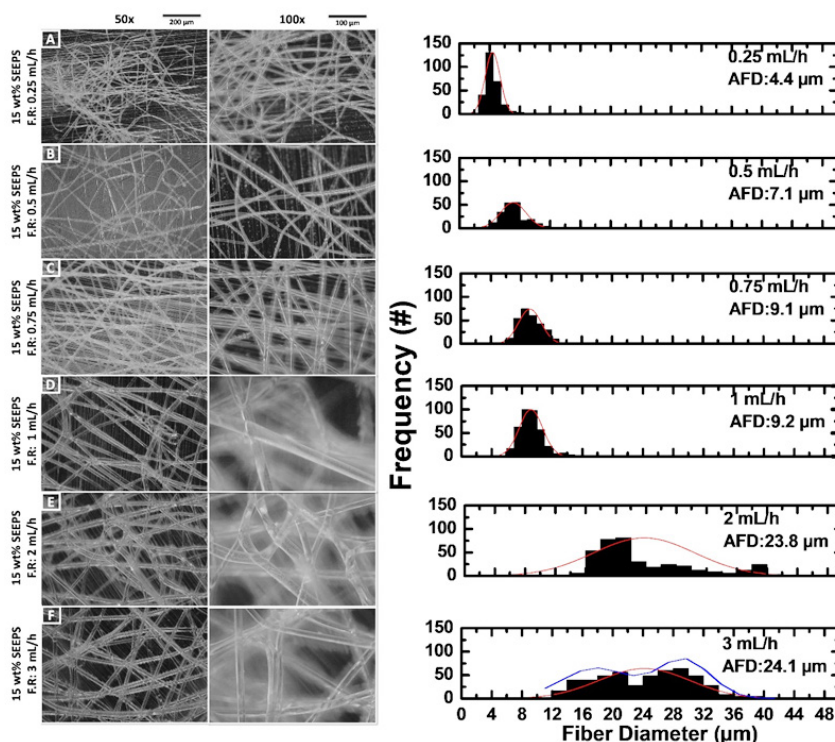


Fig. 5: Optical microscope images of electrospun samples from 15 wt% SEEPS solution (S18-S23) at 50x and 100x under different feed rates and corresponding fiber diameter distribution histograms. *F.R: Feed Rate, *AFD: Average fiber diameter

In order to observe the effect of feed rate on fiber morphology and diameter, fiber distribution histograms were also drawn (Fig.5). The averaged diameters of the fibers were calculated as 4.4, 7.1, 9.1, 9.2, 23.8, 24.1 µm for S18-S23, respectively. As obvious from the outcomes, fiber diameter increased by increasing the flow rate. From Fig. 5, fiber diameter values shifted to the right with the increasing feed rate. Also, standard deviation of fiber diameter was increased from 1 µm to 6.7 µm with the increasing feed rate. Higher feed rate caused to higher amount of polymer solution between needle and collector.

At constant electrical field, amount of stretching was lowest for the highest feed rate. In other words, the level of stretching was lower in the case of higher feed rates, fiber jet could not be stretched, and diameter became larger. This phenomenon is obvious for S23. When fiber distribution histogram was checked, distribution shifts from normal distribution to bimodal distribution. This might be attributed to increased electric current resulting in reduction of surface charge density leading to merged fiber production with the increased feed rate.³⁸ Which means that drawing ratio is changing from steady to unsteady and controlling of polymer jet between needle and

collector was getting harder with the increased feed rate. Although fiber morphology was observed for 12 and 15 wt% SEEPS solutions, more homogeneous fibers were obtained for 15 wt%. It was assumed to be caused by the viscosity of the spinning solution. Since thermoplastic elastomers are flexible polymers some level of solution viscosity is required to obtain homogeneous fiber morphology. In the future studies, average fiber diameter might be reduced under 1 μm by increasing solution conductivity with ionic salt addition; by changing collector type to rotating drum or by using ternary solvents instead of binary solvents.

Conclusions

In this study electrospinning of SEEPS block copolymer was carried out for the first time in literature. 8, 10, 12, and 15 wt% SEEPS solutions were prepared and electrospun at various conditions. It was observed that some level of viscosity is required for the fiber formation. After this value, fibers can be formed, and the fiber morphology is tunable by changing the electrospinning process parameters. Solution viscosity was found significant in terms of spinnability and 15 wt% SEEPS

containing spinning solution was determined as the optimum for obtaining a homogeneous fiber morphology. After determination of the optimum solution, various feed rates were used to tune the fiber morphology. By increasing the feed rate fiber diameter increased significantly. While the average fiber diameter was 4.4 μm under 0.25 mL h^{-1} feed rate, it was determined as around 24 μm under 3 mL h^{-1} . Also, broader fiber distribution histograms were obtained with increasing feed rate. Flexible nonwoven mats can be used for many applications from flexible filters to medical implants. Future studies will focus on various applications of SEEPS based flexible nonwoven mats.

Acknowledgment

The author would like to thank Yalova University and co-authors for their support.

Funding

The author declares that the funding is done by the author only.

Conflict of Interest

There is no conflict of interest.

Reference

1. Drobny, J. G. (2014): Handbook of Thermoplastic Elastomers 2nd ed.; William Andrew Publishing: Oxford.
2. Ma, M., Hill, R. M., Lowery, J. L., Fridrikh, S. V., Rutledge, G. C., Electrospun Poly (Styrene-block-dimethylsiloxane) Block Copolymer Fibers Exhibiting Superhydrophobicity. *Langmuir*.21 (12), 5549-5554 (2005).
3. Ruotsalainen, T., Turku, J., Heikkilä, P., Ruokolainen, J., Nykanen, A., Laitinen, T., Torkkeli, M., Serimaa, R., ten Brinke, G., Harlin, A., Ikkala, O., Towards Internal Structuring of Electrospun Fibers by Hierarchical Self-Assembly of Polymeric Comb-Shaped Supramolecules. *Advanced Materials*.17 (8), 1048-1052 (2005).
4. Kalra, V., Kakad, P. A., Mendez, S., Ivannikov, T., Kamperman, M., Joo, Y. L., Self-Assembled Structures in Electrospun Poly(styrene-block-isoprene) Fibers. *Macromolecules*. 39 (16), 5453-5457 (2006).
5. Chuangchote, S., Sirivat, A., Supaphol, P., Electrospinning of Styrene-Isoprene Copolymeric Thermoplastic Elastomers. *Polymer Journal*.38 (9), 961-969 (2006).
6. Feng, S.-Q., Shen, X.-Y., Fu, Z.-Y., Ji, Y.-L., Studies on the electrospun submicron fibers of SIS and its mechanical properties. *Journal of Applied Polymer Science*. 114 (3), 1580-1586 (2009).
7. Fong, H., Reneker, D. H., Elastomeric nanofibers of styrene-butadiene-styrene triblock copolymer. *Journal of Polymer Science Part B: Polymer Physics*. 37 (24), 3488-3493 (1999).
8. Fan, L., Xu, Y., Zhou, X., Chen, F., Fu, Q., Effect of salt concentration in spinning solution on fiber diameter and mechanical property of electrospun styrene-butadiene-styrene tri-block copolymer membrane. *Polymer*. 153, 61-69 (2018).
9. Ribeiro, S., Costa, P., Ribeiro, C., Sencadas, V., Botelho, G., Lanceros-Mendez, S., Electrospun styrene-butadiene-styrene

- elastomer copolymers for tissue engineering applications: Effect of butadiene/styrene ratio, block structure, hydrogenation and carbon nanotube loading on physical properties and cytotoxicity. *Composites Part B: Engineering*.67, 30-38 (2014).
10. Spurcaci, B.,Iancu, L.,Filipescu, M.,Ion, R.-M.,Ghioca, P.,Grigorescu, R.,Nicolae, C.,Gabor, R.,Rapa, M.,Matei, E., Polymeric Nanofibers Manufactured by Electrospinning of Styrene-Ethylene-Butylene-Styrene (SEBS) Composites. *Proceedings*. 29 (1), 84 (2019).
 11. Wang, W.,Lu, Z.,Cao, Y.,Chen, J.,Wang, J.,Zheng, Q., Investigation and prediction on the nonlinear viscoelastic behaviors of nylon1212 toughened with elastomer. *Journal of Applied Polymer Science*. 123 (3), 1283-1292 (2012).
 12. Wang, W.,Cao, Y.,Wang, J.,Zheng, Q., The gelation behaviors of the reactive blends of nylon1212 and functional elastomer. *Journal of Materials Science*. 43 (17), 5755-5762 (2008).
 13. Wang, W.,Shangguan, Y.,Zhao, L.,Yu, J.,He, L.,Tan, H.,Zheng, Q., The linear viscoelastic behaviors of Nylon1212 blends toughened with elastomer. *Journal of Applied Polymer Science*.108 (3), 1744-1754 (2008).
 14. Lin, X.,Qian, Q.,Xiao, L.,Huang, Q.,Zhou, W.,Chen, Q.,Zhang, H., Melt rheology and properties of compatibilized recycled poly(ethylene terephthalate)/(styrene-ethylene-ethylene-propylene-styrene) block copolymer blends. *Journal of Vinyl and Additive Technology*.22 (3), 342-349 (2016).
 15. Lu, Y.,Yang, Y.,Xiao, P.,Feng, Y.,Liu, L.,Tian, M.,Li, X.,Zhang, L., Effect of interfacial enhancing on morphology, mechanical, and rheological properties of polypropylene-ground tire rubber powder blends. *Journal of Applied Polymer Science*. 134 (40), 45354 (2017).
 16. Alanalp, M. B.,Durmus, A., Quantifying microstructural, thermal, mechanical and solid-state viscoelastic properties of polyolefin blend type thermoplastic elastomer compounds. *Polymer*.142, 267-276 (2018).
 17. Xanthos, M.,Chandavas, C.,Sirkar, K. K.,Gogos, C. G., Melt processed microporous films from compatibilized immiscible blends with potential as membranes. *Polymer Engineering & Science*. 42 (4), 810-825 (2002).
 18. Durmus, A.,Alanalp, M. B.,Aydin, I., Investigation of rheological behaviors of polyolefin blend type thermoplastic elastomers for quantifying microstructure-property relationships. *Korea-Australia Rheology Journal*.31 (2), 97-110 (2019).
 19. Chandavas, C.,Xanthos, M.,Sirkar, K. K.,Gogos, C. G., Fabrication of microporous polymeric membranes by melt processing of immiscible blends. *Journal of Membrane Science*.211 (1), 167-175 (2003).
 20. Qiao, X.,Lu, X.,Li, W.,Chen, J.,Gong, X.,Yang, T.,Li, W.,Sun, K.,Chen, X., Microstructure and magnetorheological properties of the thermoplastic magnetorheological elastomer composites containing modified carbonyl iron particles and poly(styrene-ethylene-ethylene-propylene-b-styrene) matrix. *Smart Materials and Structures*. 21 (11), 115028 (2012).
 21. Aoki, Y.,Takahashi, R.,Nishitsuji, S.,Ishigami, A.,Koda, T.,Nishioka, A., Viscoelasticity and morphology of polystyrene-block-poly[ethylene-co-(ethylene-propylene)]-block-polystyrene tri-block copolymer/paraffinic oil blends. 1. Effect of oil content. *Rheologica Acta*.55 (4), 293-301 (2016).
 22. Nishioka, A.,Aoki, Y.,Suzuki, T.,Ishigami, A.,Endo, T.,Koda, T.,Koyama, K., Dynamic mechanical properties of polystyrene-block-poly[ethylene-co-(ethylene-propylene)]-block-polystyrene triblock copolymer/ hydrocarbon oil blends. *Journal of Applied Polymer Science*.121 (5), 3001-3006 (2011).
 23. Takahashi, R.,Nishioka, A.,Ishigami, A.,Suzuki, T.,Nishitsuji, S.,Koda, T.,Aoki, Y., Rheology of Polystyrene-block-poly[ethylene-co-(ethylene-propylene)]-block-polystyrene Tri-block Copolymer/Paraffinic Oil Blends - Effect of Oil Molecular Weight on the Order-Disorder Transition. *Nihon Reoroji Gakkaishi*.40 (4), 171-177 (2012).
 24. Zheng, Q.,Wang, W.,Yu, Q.,Yu, J.,He, L.,Tan, H., Nonlinear viscoelastic behavior of styrene-[ethylene-(ethylene-propylene)]-styrene block copolymer. *Journal of Polymer Science Part B: Polymer Physics*. 44 (9), 1309-1319 (2006).

25. Wang, W.,Zheng, Q.,Yu, Q., Study on the viscoelastic behavior of SEEPS block copolymer based on a modified BSW model. *Chinese Science Bulletin*. 50 (19), 2171-2175 (2005).
26. Xiaoli, W.,Sizhu, W.,Kejian, W., Thermal Analysis Kinetics of the Chemical Crosslinking Reaction of the Styrene-Based Block Copolymer SEEPS. *Current Physical Chemistry*.1 (1), 65-68 (2011).
27. Karahan Toprakci, H. A.,Turgut, A.,Toprakci, O., Nailed-bat like halloysite nanotube filled polyamide 6, 6 nanofibers by electrospinning. *Polymer-Plastics Technology and Materials*. 60 (5), 520-533 (2021).
28. Toprakci, O.,Toprakci, H. A.,Ji, L.,Lin, Z.,Gu, R.,Zhang, X., Journal of Renewable,Energy, S., LiFePO₄ nanoparticles encapsulated in graphene-containing carbon nanofibers for use as energy storage materials. 4 (1), 013121 (2012).
29. Ren, M.,Zhou, Y.,Wang, Y.,Zheng, G.,Dai, K.,Liu, C.,Shen, C., Highly stretchable and durable strain sensor based on carbon nanotubes decorated thermoplastic polyurethane fibrous network with aligned wave-like structure. *Chemical Engineering Journal*.360, 762-777 (2019).
30. Emad Abdulousefi, H.,Honarasa, G., Fabrication of polyurethane and thermoplastic polyurethane nanofiber by controlling the electrospinning parameters. *Materials Research Express*.4 (10), 105308 (2017).
31. Mi, H.-Y.,Jing, X.,Salick, M. R.,Cordie, T. M.,Peng, X.-F.,Turng, L.-S., Properties and fibroblast cellular response of soft and hard thermoplastic polyurethane electrospun nanofibrous scaffolds. *Journal of Biomedical Materials Research Part B: Applied Biomaterials*.103 (5), 960-970 (2015).
32. Hansen, C. M. (2007): Hansen Solubility Parameters: A User's Handbook. Second Edition ed.; CRC Press: Boca Raton FL, USA.
33. Ovejero, G.,Pérez, P.,Romero, M. D.,Díaz, I.,Díez, E., SEBS triblock copolymer-solvent interaction parameters from inverse gas chromatography measurements. *European Polymer Journal*.45 (2), 590-594 (2009).
34. Peng, W.,Shuhua, Q.,Nailiang, L.,Kangqing, D.,Haiying, N., Investigation of Thermodynamic Properties of SIS, SEBS, and Naphthenic Oil by Inverse Gas Chromatography. *Journal of Elastomers & Plastics*.43 (4), 369-386 (2011).
35. Poleo, E. E.,Daugulis, A. J., A comparison of three first principles methods for predicting solute-polymer affinity, and the simultaneous biodegradation of phenol and butyl acetate in a two-phase partitioning bioreactor. *Journal of Chemical Technology & Biotechnology*. 89 (1), 88-96 (2014).
36. Politakos, N.,Kortaberria, G., Exploring the Self-Assembly Capabilities of ABA-Type SBS, SIS, and Their Analogous Hydrogenated Copolymers onto Different Nanostructures Using Atomic Force Microscopy. *Materials*. 11 (9), (2018).
37. Mahmud, M. M.,Perveen, A.,Matin, M. A.,Arafat, M. T., Effects of binary solvent mixtures on the electrospinning behavior of poly (vinyl alcohol). *Materials Research Express*.5 (11), 115407 (2018).
38. Nauman, S.,Lubineau, G.,Alharbi, H. F., Post Processing Strategies for the Enhancement of Mechanical Properties of ENMs (Electrospun Nanofibrous Membranes): A Review. *Membranes*.11 (1), (2021).